

Influence of strain, surface diffusion and Ostwald ripening on the evolution of nanostructures for erbium on Si(001)

Cite as: Journal of Applied Physics **93**, 4180 (2003); <https://doi.org/10.1063/1.1557787>
Submitted: 23 July 2002 • Accepted: 08 January 2003 • Published Online: 21 March 2003

Lena Fitting, M. C. Zeman, W.-C. Yang, et al.



View Online



Export Citation

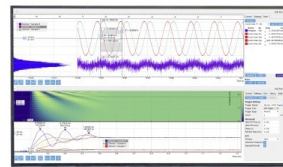
ARTICLES YOU MAY BE INTERESTED IN

[Role of Ostwald ripening in islanding processes](#)

Applied Physics Letters **51**, 975 (1987); <https://doi.org/10.1063/1.98781>

Challenge us.

What are your needs for
periodic signal detection?



Zurich
Instruments

Influence of strain, surface diffusion and Ostwald ripening on the evolution of nanostructures for erbium on Si(001)

Lena Fitting, M. C. Zeman, W.-C. Yang, and R. J. Nemanich^{a)}

Department of Physics, North Carolina State University, Raleigh, North Carolina 27695-8202

(Received 23 July 2002; accepted 8 January 2003)

This study explores the evolution of nanoscale islands and wire structures during deposition and surface ripening. Ultraviolet photoelectron emission microscopy has been employed to study the real time growth process of individual erbium silicide nanostructures on Si(001) surfaces at temperatures up to 1050 °C. During the initial island formation process compact islands form and some undergo a shape transition to elongated islands oriented along the $\langle 110 \rangle$ directions of the Si substrate. The initial island formation is driven by the surface and interface energies of the silicide/Si structure. The widths of the growing islands remain essentially constant while the lengths increase. The observed elongated islands are ~ 150 nm wide, which is larger than the width of prior reported erbium silicide nanowire structures. We propose that the ~ 150 nm elongated islands are partially relaxed, possibly through the formation of misfit dislocations. The results indicate a temperature regime where island growth is mainly governed by surface diffusion of the deposited Er adatoms and a higher temperature regime where Ostwald ripening contributes to the island morphology. © 2003 American Institute of Physics. [DOI: 10.1063/1.1557787]

I. INTRODUCTION

As the dimensions of micro- and optoelectronic devices continue to shrink and the number of devices increases, new approaches for device structures and fabrication have been considered. An alternative approach to conventional lithography techniques is the spontaneous self-assembly of nanoscale structures during epitaxial growth.¹⁻³

It has been shown that strained layers are unstable against shape changes such as the formation of islands.⁴ These shape changes constitute a major mechanism for strain relaxation. Tersoff *et al.*⁵ derived an expression for the energy of dislocation-free strained islands. The authors showed that strained islands, as they increase in size, may undergo a shape transition to elongated islands, which allows a better relaxation of the island's stress. Hence, in heteroepitaxy self-assembled quasi-one-dimensional quantum wires can form. In the case of anisotropic stress, the islands grow perpendicular to the direction of maximum stress, i.e., in the direction of minimum lattice mismatch, which minimizes the strain energy.⁵

Several studies have shown that rare earth metal silicide nanowires can be grown by metal deposition on silicon.^{2,3} In this study we investigate the system of erbium deposited on Si(001) surfaces. ErSi₂ layers grow on Si(001) with hexagonal or tetragonal crystalline structures, depending on the method of deposition, the substrate temperature, and their stoichiometry.^{6,7}

The tetragonal phase of ErSi₂ has a ThSi₂ type structure with lattice parameters $a = b = 3.96$ Å and $c = 13.26$ Å. On Si(001) the tetragonal phase of ErSi₂ grows with $[001]_{\text{ErSi}_2}$ and $[010]_{\text{ErSi}_2}$ parallel to the $\langle 110 \rangle_{\text{Si}}$ axes and with $(100)_{\text{ErSi}_2} // (001)_{\text{Si}}$.^{6,7} Hence the lattice mismatch between

tetragonal ErSi₂ and Si along the $\langle 110 \rangle$ axes is 3%.

ErSi₂ with a hexagonal AlB₂ type structure grows with the $[0001]$ and one of the $\langle 11-20 \rangle$ axes parallel to the $\langle 110 \rangle$ axes of the Si substrate. The lattice mismatch along $[11-20]_{\text{ErSi}_2} // [110]_{\text{Si}}$ and $[0001]_{\text{ErSi}_2} // [110]_{\text{Si}}$ is -1.22% and $+6.3\%$, respectively.³ During ErSi₂ growth on Si(001), the lattice mismatch strain increases faster along the direction of larger mismatch, i.e., along the $[0001]_{\text{ErSi}_2}$ direction. To minimize the strain energy, the crystals grow preferentially in the $[11-20]_{\text{ErSi}_2}$ direction, resulting in nanoscale wires aligned along the two equivalent $\langle 110 \rangle_{\text{Si}}$ directions. Prior work has shown ErSi₂ wires with hexagonal crystalline structures of the order of 5 nm in width, 1 nm in height, and with varying length up to 500 nm.²

However, experimental data of these nanowires usually involves scanning probe measurements after the growth has proceeded for a fixed time. In order to understand the growth mechanism, it is necessary to study the evolution of individual islands and groups of islands using *in situ* real-time microscopy techniques.

In this study we employ real-time photoelectron emission microscopy (PEEM) measurements to monitor the evolution of the surface and individual islands during *in situ* erbium deposition and annealing. In particular, we observe the transition from compact islands into wire structures and their growth during deposition of Er adatoms. We find a temperature regime where the island growth is mainly governed by surface diffusion of the deposited species and a regime where coarsening processes also contribute to the growth morphology.

II. EXPERIMENTAL PROCEDURE

The nanostructures are grown *in situ* by Er deposition on silicon in ultrahigh vacuum (UHV). The Si(001) substrates

^{a)}Electronic mail: robert_nemanich@ncsu.edu

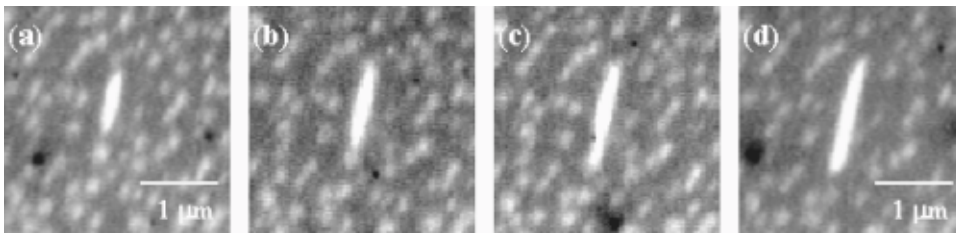


FIG. 1. Sequential PEEM images of the evolution of a 10–20 Å Er layer deposited at 750 °C during annealing at 800 °C for (a) 23 min, (b) 31 min, (c) 37 min, and (d) 45 min, respectively.

were cleaned by UV-ozone exposure and a wet chemical clean using a 10:1 hydrofluoric acid solution diluted in deionized water. After *ex situ* cleaning, the wafers were introduced into the UHV system through a load lock and submitted to a thermal treatment at 900 °C for 10 min. Auger electron spectroscopy (AES) and low energy electron diffraction (LEED) were used to confirm that the preparation technique was sufficient. LEED showed a sharp (2×1) reconstruction of the Si(001) surface, and AES showed less than 1% carbon and 2% oxygen on the cleaned surface. The experiments were carried out using an UHV PEEM system (Elmitech) with a base pressure $< 2\times 10^{-10}$ Torr. Two separate UV sources were employed to excite the photoemission. A 100 W-Hg discharge lamp with an upper cutoff energy near 4.9 eV was used for most experiments. The tunable UV free electron laser (UV-FEL) at the Duke University Free Electron Laser Laboratory allowed us to use photons in the 3–7 eV energy range and thus to maximize the sample contrast. We obtained a contrast maximum at 4.9 eV, which is close to the photon cutoff energy of the Hg lamp. Details of the UV-FEL PEEM system have been described previously.⁸

Erbium was deposited from an *in situ* electron-beam evaporator at substrate temperatures ranging from room temperature to 800 °C. After deposition, the samples were annealed at temperatures up to 1050 °C. The real-time surface evolution was observed with *in situ* PEEM. The images displayed with a microchannel plate and a phosphor screen are monitored with a charge coupled device camera and stored digitally with an image processor. For the data presented here, 16 successive images were integrated.

III. RESULTS AND DISCUSSION

A. Initial island formation

Figure 1 shows a sequence of PEEM images obtained during the annealing process after the deposition of a 10–20 Å thick Er layer at 800 °C. The ErSi_2 islands are identified as the bright spots in the images while the Si surface appears as the darker region. The PEEM image contrast is due to the difference in the photothreshold of ErSi_2 (4.8 eV)⁹ and Si. For Si(111), the photothreshold is approximately 5.15 eV¹⁰ which we assume is close to the value for the Si(001) surface.

Prior studies of the growth of erbium silicide films on Si(001) by Travlos *et al.*⁶ have shown that ErSi_2 forms at temperatures as low as 450 °C. Here, we deposited Er at a substrate temperature of 750 °C; thus we anticipate that Er reacts with the Si substrate to form erbium silicide. Starting with an erbium silicide covered surface, compact islands form at temperatures below 800 °C. The initial island forma-

tion is most likely driven by the surface and interface energies of the silicide/Si structure. During the annealing process the ErSi_2 diffuses on the surface, and the islands form due to surface energies and coalescence of nearby islands.

We also observed specific islands that undergo a shape transition from compact to elongated morphology. Figure 2 shows the evolution of the dimensions of an individual island (from Fig. 1) during the early stage growth after the erbium deposition. The island grows only in one direction, i.e., the length increases while the width in the perpendicular direction remains essentially constant. This observation is in agreement with the model by Tersoff and Tromp⁵ for shape transition of strained epitaxial islands. However, we could not monitor the evolution of the length and the width around the transition point. Following the model of Tersoff and Tromp, we anticipate that compact erbium silicide epitaxial islands should grow up to a critical size $e\alpha_0$. At this size the shape transition occurs, and further growth results in a reduction of the width to the optimal size α_0 and an increase of the length.⁵ Thus beyond the critical size the epitaxial erbium silicide islands elongate, and during the later stage growth the width remains essentially constant. However, nonepitaxial islands do not elongate but grow in all directions. During the annealing process the nanostructures grow, resulting in a surface covered with compact islands and elongated island structures.

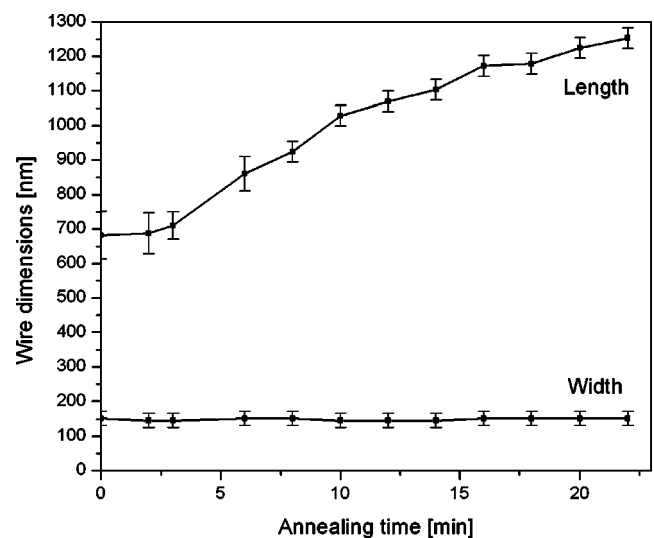


FIG. 2. Evolution of the dimensions of an individual wire during the annealing process in Fig. 1. The length increases while the width remains essentially constant.

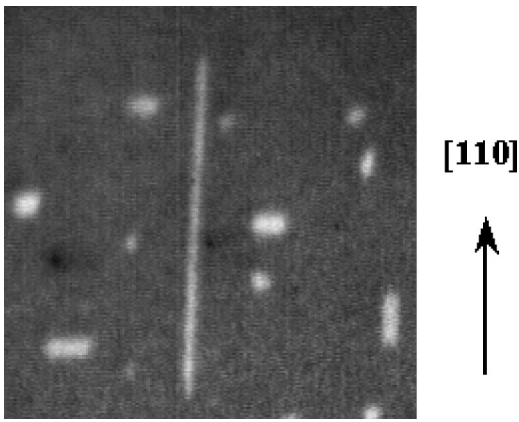


FIG. 3. PEEM image of a nanowire (length: $4.84 \mu\text{m}$; width: $0.16 \mu\text{m}$) aligned along the $[110]$ direction after 60 min of continuous Er deposition (field of view: $5.88 \mu\text{m}$).

B. Surface evolution during deposition

Following the initial annealing, we investigated the surface evolution during continuous Er deposition on the island formed surface. The Er deposition was initiated at a low rate with the sample at 800°C . The nucleation of additional islands was not observed. Instead, existing islands grew through absorption of Er adatoms (supplied from the Er flux) and reaction with Si from the surface. This indicates that the Er adatoms diffuse rapidly on the surface, and have a low probability of forming critical nuclei.

During the continuous deposition of Er on the surface, the length of the erbium silicide wires increases, while the width does not change significantly. Given the randomness of diffusion, it is reasonable to presume that Er adatoms diffuse not only to the ends of the wires, but also to the edges. Thus, either the Er adatoms do not attach to the edges but only the ends of the wire, or after the attachment at the edges they diffuse rapidly to the ends, resulting in the further elongation of the wire. Given the large chemical energy of forming the silicide, it seems most likely that the Er atoms collect on the islands edges and then rapidly diffuse to the ends where growth is preferred due to the strain energy considerations.

At this point we have only considered the diffusion of the Er atoms. Our assumption is that there is always a source or sink of Si, which is supplied through reaction with the substrate or from Si adatoms supplied from nearby step edges.

With the Er source off, the surface remained unchanged during annealing at 800°C . Under these conditions, we did not observe coarsening processes, i.e., Ostwald ripening and coalescence, within a time range of 30 min. Thus, at temperatures around 800°C the later stage island growth is governed by incorporation of the deposited Er adatoms through rapid diffusion.

After all processing in the PEEM, the surfaces were examined using an atomic force microscope (AFM), and the wire dimensions measured. Figure 3 shows an elongated island with an aspect ratio of 30:1 (length: $4.84 \mu\text{m}$ and width: $0.16 \mu\text{m}$) aligned along the $[110]$ direction of the Si substrate. After 60 min of continuous Er deposition the elon-

gated islands were $2\text{--}5.5 \mu\text{m}$ long, $140\text{--}180 \text{ nm}$ wide, and $13\text{--}17 \text{ nm}$ high. Note that the width of all observed elongated islands were of the order of 150 nm , which is much larger than the prior reported widths of about 5 nm for hexagonal ErSi_2 nanowires. However, our elongated islands have some similarities with the Er silicide islands recently reported by Chen *et al.*¹¹ In their study, they produced a rather dense pattern of wires by deposition of $\sim 4 \text{ nm}$ of Er at room temperature and annealing to 700°C . Their islands were found to exhibit the tetragonal structure and were aligned along the $\langle 110 \rangle$ directions of the Si. At this time we have not established whether our ErSi_2 island are of the tetragonal phase with a 3% mismatch or the hexagonal phase with a -1.22% and $+6.3\%$ mismatch between ErSi_2 and Si in the $\langle 110 \rangle_{\text{Si}}$ directions, respectively.

Brongersma *et al.*¹² reported observation of the shape transition of CoSi_2 islands on $\text{Si}(001)$. Their results were analyzed based on the theoretical model of Tersoff and Tromp⁵ for a shape transition during the growth of strained islands. The lattice mismatch of CoSi_2 on $\text{Si}(001)$ is $\sim 1.2\%$, hence, the epitaxial islands are strained. The model of Tersoff and Tromp balances the surface and interface energies due to the island formation with the energy change due to island relaxation obtained by elastic distortion. As described in Ref. 5, minimization of the island energy per unit volume with respect to the width and the length of the island yields an optimal size, α_0 , which is given by

$$\alpha_0 = e \phi h e^{\Gamma/ch},$$

where h is the islands height, $\phi = e^{-3/2} \cot \theta$, and θ is the islands contact angle. For fixed θ and h , the critical size is determined by the ratio of surface energy and island strain energy (Γ/ch). The constant c depends on the island bulk stress, the Poisson ratio, and the shear modulus of the substrate. If the surface energy Γ dominates, then the critical size becomes large. However, if the island strain energy is increased relative to the surface energy, then the minimum energy is obtained with smaller islands. Hence an increase in the substrate–island strain results in a reduction of the optimal size α_0 of the elongated epitaxial islands.

Following this model, Brongersma *et al.*¹² measured an optimal size, α_0 , of 68 nm for their CoSi_2 islands on $\text{Si}(001)$ by fitting the theoretical model to their experimental results. The lattice mismatch for ErSi_2 islands on $\text{Si}(001)$ is $\sim 3\%$ for the tetragonal phase and -1.22% and $+6.3\%$ for the hexagonal phase. Hence the lattice mismatch strain energy for ErSi_2 island is expected to be larger than for CoSi_2 islands on $\text{Si}(001)$. Assuming that the surface and the interface energies for CoSi_2 and ErSi_2 island formation are comparable, then α_0 should be smaller for ErSi_2 and the elongated islands are expected to be narrower. However, the width of 150 nm observed for our elongated islands indicates that the strain term, ch , is smaller than expected based on comparison with CoSi_2 .

We propose that erbium silicide islands grown at 800°C are partially relaxed through the formation of dislocations or other relaxation mechanisms such as trench formation.¹³ The relaxation leads to a reduction of the strain energy, and therefore, to an increase of the optimal size, α_0 . The ErSi_2 wires

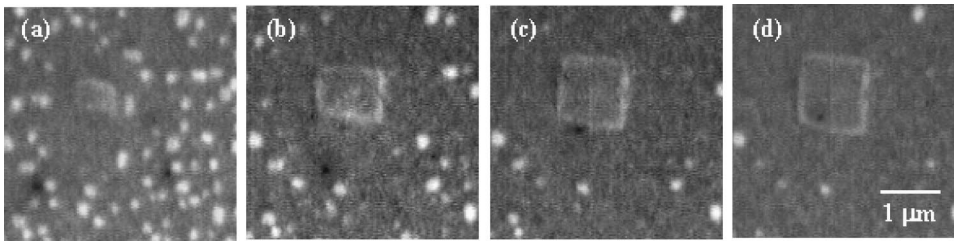


FIG. 4. Sequential PEEM images of erbium silicide island growth during annealing at 1050 °C for (a) 5 min, (b) 14 min, (c) 16 min, and (d) 18 min, respectively.

are all of similar width indicating similar strain relaxation. Hence this size represents the optimal tradeoff between surface energy and the strain due to the partially relaxed interface. It is likely that the CoSi_2 islands observed by Brongersma *et al.*¹² are also partially relaxed.

Our results suggest that there are different energy minima depending on the degree of strain relaxation. For wires that are fully strained the width of the equilibrium shape decreases to its minimum, i.e., the wires become very narrow. This corresponds well with the observations of Chen *et al.*,² which show ErSi_2 wires with widths of ~ 5 nm. Strain relaxing dislocations were not observed in the scanning tunneling microscopy images of these wires, however, different strain mechanisms may be more effective for the different sized wires.

C. Surface evolution at higher temperature

To explore the dynamics with enhanced surface diffusion, a similar experiment was performed where an ~ 2 nm thick Er film was annealed at 1050 °C. As the annealing time increased, the average size of the islands increased while the number of islands decreased. Figure 4 shows a large island growing larger and smaller islands disappearing during the annealing process. This is characteristic of Ostwald ripening where larger islands grow at the expense of smaller islands. In the ripening process atoms detach from small islands, diffuse through the adatom sea surrounding the islands, and attach to larger islands. The growth behavior of an individual island depends on the chemical potential of the surrounding adatom sea, the chemical potential of the atoms in the island, and the barrier for detachment and attachment. If the exchange between the adatom sea and the island edge is sufficiently rapid, then the net flow of adatoms towards or away from the island is determined by diffusion in the chemical potential gradient of the adatom sea. On the other hand, if the

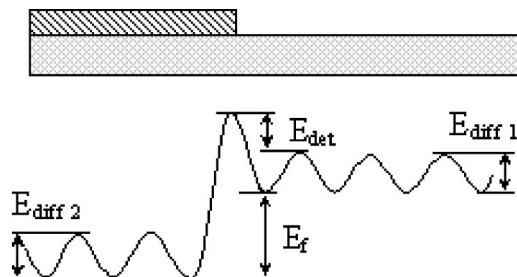


FIG. 5. Simplified diagram of surface activation barriers near an island step edge. $E_{\text{diff } 1/2}$ are the diffusion barriers on the substrate and on the island, respectively. E_f is the adatom formation energy, and E_{det} is the attachment/detachment barrier.

detachment and attachment is slow in comparison to diffusion, then the adatom detachment/attachment is the rate-limiting step for coarsening. This case is realized if there is an additional activation barrier E_{det} that the detaching atoms have to overcome. Figure 5 is a schematic diagram of the energy barriers near an island step edge. In the diffusion limited regime the activation energy is $E_a \approx E_{\text{diff } 1}$; whereas in the attachment/detachment limited regime the activation energy is $E_a \approx E_{\text{det}} + E_f$.¹⁴ Here, $E_{\text{diff } 1}$ is the adatom surface diffusion barrier on the substrate, E_f the adatom formation energy, and E_{det} the barrier for adatom detachment/attachment.

Lifshitz and Sloyozov¹⁵ first considered Ostwald ripening of three-dimensional (3D) clusters in a 3D environment for the diffusion limited regime. Wagner¹⁶ extended the theory to include the case that the transfer of adatoms between the cluster and the environment is the limiting process. Further studies by Wynblatt *et al.*¹⁷ and others¹⁸ applied the theory to 2D and 3D clusters on surfaces. In all cases, the ripening processes can be described by the relation: $A \propto t^n$, where A is the island area and t is the time. The exponent n is $2/3$ for diffusion-limited ripening and 1 if the ripening is detachment/attachment limited.^{16–19} Figure 6 shows the evolution of the squared island area from Fig. 4 during the ripening process. As a best fit, we obtained an exponent of 1.29 ± 0.07 which indicates that diffusion is not the rate limiting mechanism for this system. The ripening of ErSi_2 nano-

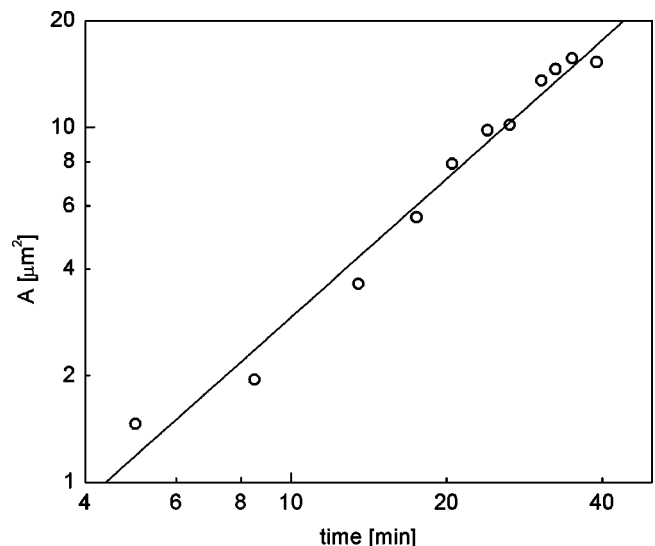


FIG. 6. Time dependence of the island area (A) in Fig. 4 during ripening at 1050 °C. The linear fit yields $\log(A) \propto 1.3 \log(t)$ which indicates an attachment/detachment limited growth mechanism.

structures grown on Si(001) is mainly limited by detachment/attachment of adatoms from island edges, and controlled by the barrier $E_f + E_{\text{det}}$. The deviation of the exponent from the value 1 for attachment/detachment limited ripening implies that other mechanisms such as evaporation could play an important role. Note that this result is based on the investigation of a single island, and further measurements are necessary to more accurately define the dynamics.

At 800 °C Ostwald ripening was not observed which indicates that the detachment of adatoms is very slow at this temperature. However, when erbium adatoms are deposited they only have to overcome the surface diffusion barrier. Thus the deposited adatoms diffuse on the surface and ErSi₂ nanostructures grow. In contrast, at 1050 °C coarsening processes were observed. The small islands disappear due to ripening, and the relatively large rectangular islands remain on the surface. We propose that the formation of these rectangular islands at 1050 °C is due to a further reduction of the strain energy. At elevated temperatures the strain relaxation, for example, through the generation of misfit dislocations, is promoted.^{20,21} For instance, at 1050 °C the density of dislocations in the erbium silicide islands would increase leading to further relaxation of the strained islands. The surface energy dominates, and the tendency to elongate is reduced. Additional experiments including transmission electron microscopy measurements are necessary to reinforce this point.

IV. CONCLUSIONS

We have utilized real-time PEEM to observe the evolution of erbium silicide nanostructures on Si(001) during high-temperature annealing and deposition of Er. By monitoring individual islands during the annealing process, we observed the growth of elongated islands with time. During Er deposition the length of these elongated islands increases while the width remains constant. The width of our observed erbium silicide elongated island was measured to be ~150 nm, which is much larger than the prior reported nano islands with a width of ~5 nm. We propose that the ~150 nm elongated islands are partially relaxed, possibly through the formation of misfit dislocations. The strain relaxation results in an increase of the width of the wire. We suggest that the width will depend on the strain relaxation at the interface with narrower structures at more highly strained interfaces and wider structures at more completely relaxed interfaces. At temperatures of ~800 °C the island growth is governed

by surface diffusion of the deposited Er adatoms, and Ostwald ripening processes do not contribute to the evolution of the island morphology. Increasing the annealing temperature to 1050 °C, Ostwald ripening and coalescence of islands contributes to the evolution of the surface morphology. The results presented here demonstrate that control of interface strain and kinetic effects can lead to engineered island structures.

ACKNOWLEDGMENTS

This research is supported by the National Science Foundation, the Tera-level Nano Devices program of the Republic of Korea, and the DOD MFEL program administered by Air Force Office of Scientific Research. The authors gratefully acknowledge the support of the Duke University Free Electron Laser Laboratory.

- ¹H. Omi and T. Ogino, *Appl. Phys. Lett.* **71**, 2163 (1997).
- ²Y. Chen, D. A. A. Ohlberg, and R. S. Williams, *Mater. Sci. Eng., B* **87**, 224 (2001).
- ³J. Nogami, B. Z. Liu, M. V. Katkov, C. Ohbuchi, and N. O. Birge, *Phys. Rev. B* **63**, 233305 (2001).
- ⁴B. J. Spencer, P. W. Voorhees, and S. H. Davis, *Phys. Rev. Lett.* **67**, 3696 (1991).
- ⁵J. Tersoff and R. M. Tromp, *Phys. Rev. Lett.* **70**, 2782 (1993).
- ⁶A. Travlos, N. Salamouras, and E. Flouda, *Appl. Surf. Sci.* **120**, 355 (1997).
- ⁷N. Frangis, J. Van Landuyt, G. Kaltsas, A. Travlos, and A. G. Nassiopoulou, *J. Cryst. Growth* **172**, 175 (1997).
- ⁸H. Ade, W. Yang, S. English, J. Hartman, R. F. Davis, R. J. Nemanich, V. N. Litvinenko, I. V. Pinayev, Y. Wu, and J. M. Mady, *Surf. Rev. Lett.* **5**, 1257 (1998).
- ⁹A. Siokou, S. Kennou, and S. Ladas, *Surf. Sci.* **331-333**, 580 (1995).
- ¹⁰F. G. Allen and G. W. Gobeli, *Phys. Rev.* **127**, 150 (1962).
- ¹¹G. Chen, J. Wan, J. Yang, X. Ding, L. Ye, and X. Wang, *Surf. Sci.* **513**, 203 (2002).
- ¹²S. H. Brongersma, M. R. Castell, D. D. Perovic, and M. Zinke-Allmann, *Phys. Rev. Lett.* **80**, 3795 (1998).
- ¹³C. Preinesberger, S. K. Becker, S. Vandr e, T. Kalka, and M. D ahne, *J. Appl. Phys.* **91**, 1695 (2002).
- ¹⁴S. Kodambaka, V. Petrova, A. Vailionis, P. Desjardins, D. G. Cahill, I. Petrov, and J. E. Greene, *Thin Solid Films* **392**, 164 (2001).
- ¹⁵I. M. Lifshitz and V. V. Slyozov, *J. Phys. Chem. Solids* **19**, 35 (1961).
- ¹⁶C. Wagner, *Z. Elektrochem.* **65**, 581 (1961).
- ¹⁷P. Wynblatt and N. A. Gjostein, in *Progress in Solid State Chemistry Vol. 9*, edited by J. O. McCaldin and G. Somorjai (Pergamon, Oxford, 1975).
- ¹⁸J. G. McLean, B. Krishnamachari, D. R. Peale, E. Chason, J. P. Sethna, and B. H. Cooper, *Phys. Rev. B* **55**, 1811 (1997).
- ¹⁹N. C. Bartelt, W. Theis, and R. M. Tromp, *Phys. Rev. B* **54**, 11741 (1996).
- ²⁰M. Khantha and V. Vitek, *Acta Mater.* **45**, 4675 (1997).
- ²¹F. K. LeGoues, M. C. Reuter, J. Tersoff, M. Hammar, and R. M. Tromp, *Phys. Rev. Lett.* **73**, 300 (1994).